BIOCHEMISTRY
including biophysical chemistry & molecular biology

ARTICLE

pubs.acs.org/biochemistry

Mechanistic Evaluation of *MelA* α-Galactosidase from *Citrobacter freundii*: A Family 4 Glycosyl Hydrolase in Which Oxidation Is Rate-Limiting

Saswati Chakladar,[†] Lydia Cheng,[‡] Mary Choi,[†] James Liu,[‡] and Andrew J. Bennet*

[†]Department of Chemistry and [‡]Department of Molecular Biology and Biochemistry, Simon Fraser University, 8888 University Drive, Burnaby, British Columbia V5A 1S6, Canada

Supporting Information

ABSTRACT: The *MelA* gene from *Citrobacter freundii*, which encodes a glycosyl hydrolase family 4 (GH4) α-galactosidase, has been cloned and expressed in *Escherichia coli*. The recombinant enzyme catalyzes the hydrolysis of phenyl α-galactosides via a redox elimination−addition mechanism involving oxidation of the hydroxyl group at C-3 and elimination of phenol across the C-1−C-2 bond to give an enzyme-bound glycal intermediate. For optimal activity, the MelA enzyme requires two cofactors, NAD^+ and Mn^{2+}, and the addition of a reducing agent, such as mercaptoethanol. To delineate the mechanism of action for this GH4 enzyme, we measured leaving group effects, and the derived β_{lg} values on V and V/K are indistinguishable from zero (−0.01 ± 0.02 and 0.02 ± 0.04, respectively). Deuterium kinetic isotope effects (KIEs) were measured for the weakly activated substrate phenyl α-D-galactopyranoside in which isotopic substitution was incorporated at C-1, C-2, or C-3. KIEs of 1.06 ± 0.07, 0.91 ± 0.04, and 1.02 ± 0.06 were measured on V for the 1-^{2}H, 2-^{2}H, and 3-^{2}H isotopic substrates, respectively. The corresponding values on V/K were 1.13 ± 0.07, 1.74 ± 0.06, and 1.74 ± 0.05, respectively. To determine if the KIEs report on a single step or on a virtual transition state, we measured KIEs using doubly deuterated substrates. The measured $^DV/K$ KIEs for MelA-catalyzed hydrolysis of phenyl α-D-galactopyranoside on the dideuterated substrates, $^DV/K_{(3\text{-D})/(2\text{-D},3\text{-D})}$ and $^DV/K_{(2\text{-D})/(2\text{-D},3\text{-D})}$, are 1.71 ± 0.12 and 1.71 ± 0.13, respectively. In addition, the corresponding values on V, $^DV_{(3\text{-D})/(2\text{-D},3\text{-D})}$ and $^DV_{(2\text{-D})/(2\text{-D},3\text{-D})}$, are 0.91 ± 0.06 and 1.01 ± 0.06, respectively. These observations are consistent with oxidation at C-3, which occurs via the transfer of a hydride to the on-board NAD^+, being concerted with proton removal at C-2 and the fact that this step is the first irreversible step for the MelA α-galactosidase-catalyzed reactions of aryl substrates. In addition, the rate-limiting step for V_{max} must come after this irreversible step in the reaction mechanism.

Glycosidases (glycosyl hydrolases) make up an important class of carbohydrate-processing enzymes, which number more than 110 families that are classified on the basis of their protein sequence.[1] Glycosyl hydrolases (GHs) hydrolyze their respective substrates with either retention or inversion of anomeric configuration, by using a variety of catalytic strategies.[2] Most GH families use a combination of general-acid catalysis, which assists departure of the aglycone, and either nucleophilic catalysis (retaining families) or general-base catalysis of water attack at the anomeric center (inverting families). In contrast, family 4 (GH4) members, which are solely derived from bacterial sources, contain a characteristic glycine rich sequence that, in combination with the topological arrangement of the secondary structure, is consistent with a Rossmann fold, a structural motif that is primarily involved in the binding of NAD(H).[3] The crystal structure of α-glucosidase A, AglA, from *Thermotoga maritima* in a complex with NAD^+ and maltose has been determined to a resolution of 1.9 Å, where Cys-174 and neighboring histidines have been shown to be key catalytic residues.[4] Importantly, this research group suggested, on the basis of electron density maps, that Cys-174 is easily oxidized to a sulfinic acid. This observation is consistent with the noted requirement for the presence of a reducing agent such as 2-mercaptoethanol or dithiothreitol for maximal catalytic activity. Recently, another GH family (GH109) has been shown to require NAD^+ for activity.[5] In addition to the requirement for NAD^+, the catalytic activity of family 4 GHs is also dependent on the presence of a divalent metal, typically Mn^{2+}, which in the single-crystal X-ray diffraction-based structure is shown to be chelated to O-2 and O-3 of the sugar ring.[6] A detailed structural analysis of GlvA 6-phospho-α-glucosidase showed that the Mn^{2+} ion promotes association of the protein to give the active tetramer.[7] Notably, different members of GH4 possess catalytic activity against α- and β-glycosides, a characteristic not seen in members of most glycosyl hydrolase families that directly promote nucleophilic reactions at the anomeric center. Members of GH4 can hydrolyze both phosphorylated and nonphosphorylated disaccharide substrates, suggesting the possible involvement of the phosphoenolpyruvate-dependent sugar phosphotransferase system (PEP-PTS) in the species from which the gene has been isolated.[8] GH4 members also

Received: November 10, 2010
Revised: April 14, 2011
Published: April 15, 2011

Scheme 1. Current Proposal for the Mechanism of GH4 Enzymes

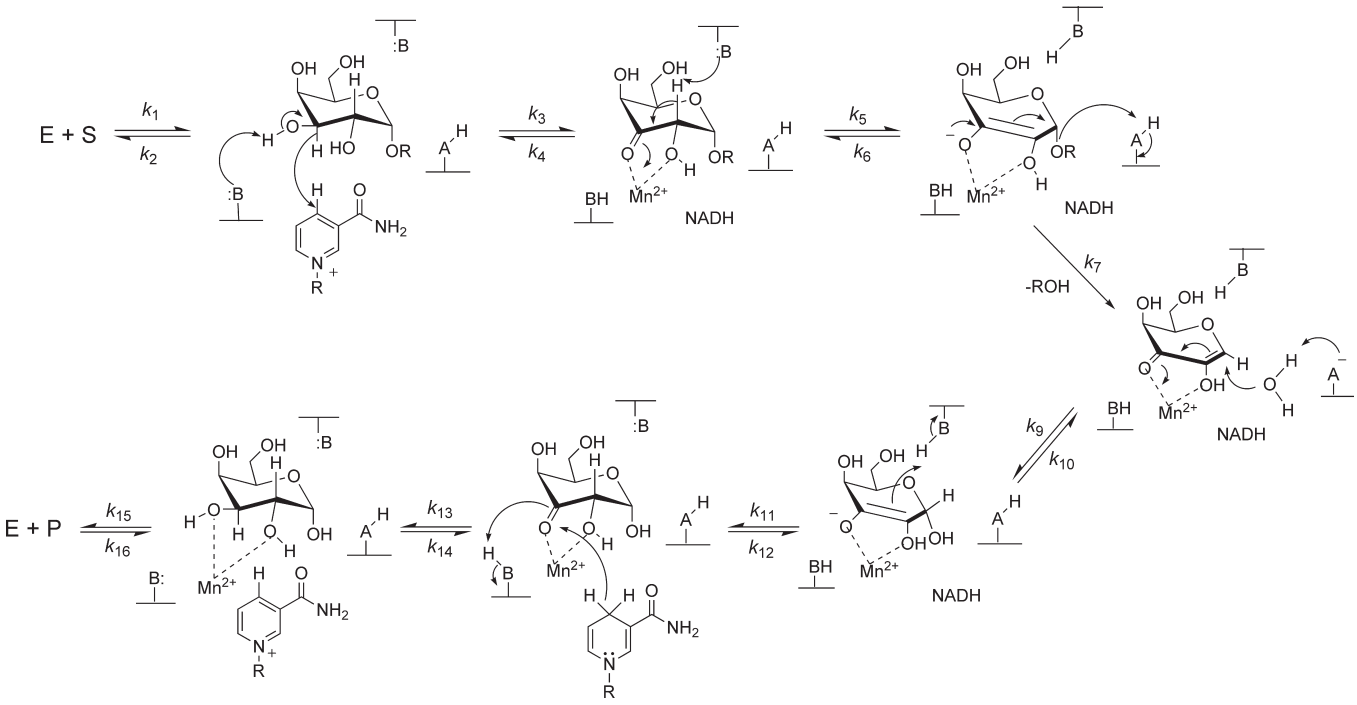

are approximately 15% similar in sequence to lactate/malate dehydrogenases.

As a result of these unusual features that are present in family 4 glycosyl hydrolases, in-depth kinetic studies have been performed to delineate the prototypical mechanism of action for this GH family. Yip et al.[6,9,10] reported such mechanistic studies on two GH4 family members, BglT from *Thermotoga maritima* and GlvA from *Bacillus subtilis*. These authors showed that GH4 members catalyze glycoside hydrolysis via an NAD^+-dependent redox reaction that is coupled to an α,β-elimination reaction involving the formation of an α,β-unsaturated ketone (glycal) intermediate.[10] Moreover, on the basis of kinetic isotope effect (KIE) measurements, they concluded that oxidation at C-3 and the subsequent C-2 deprotonation steps are both partially rate-limiting.[6,9] The proposed mechanistic outline for GH4 enzymes is depicted in Scheme 1 for an α-galactosidase.

This study details a mechanistic investigation of a GH4 α-galactosidase that is encoded by the *MelA* gene from the species *Citrobacter freundii*. This gene encodes an enzyme that hydrolyzes the terminal α-galactosyl units from glycolipids and glycoproteins. Melibiose [α-D-Gal*p*-(1→6)-D-Glc*p*] utilization in *Escherichia coli* is dependent on the melibiose locus (*Mel*), which forms an operon consisting of at least two structural genes, *MelA* and *MelB*, which encode an α-galactosidase and a melibiose carrier protein, respectively.[11] Results from identification and purification studies with *MelA* have shown it to be a tetrameric protein with a molecular mass of 200 kDa for the active enzyme.[11] In addition, Anggraeni et al.[12] showed that rMel4A α-galactosidase exhibited the highest k_{cat} values on the natural substrate melibiose but exhibited the highest affinity for raffinose.

MATERIALS AND METHODS

Materials. All chemicals were of analytical grade or better and were purchased from Sigma-Aldrich unless noted otherwise. Milli-Q water (18.2 MΩ cm^{-1}) was used for all kinetic experiments. All pH values were measured using a standard pH electrode attached to a VWR pH meter. All NMR spectra were recorded on either a Bruker 400, 500, or 600 MHz spectrometer. Chemical shifts are reported in parts per million downfield from signals for TMS. The signal residues from deuterated chloroform and external TMS salts (D_2O) were used for ^1H NMR spectral references; for ^{13}C NMR spectra, natural abundance signals from $CDCl_3$ and external TMS salts (D_2O) were used as references. Coupling constants (J) are reported in hertz. Melting points were determined on a Gallenkamp melting point apparatus and are not corrected. Optical rotations were measured on a Perkin-Elmer 341 polarimeter and are reported in units of degrees square centimeter per gram (concentrations reported in units of grams per 100 mL). All fitting of kinetic data was performed using the appropriate nonlinear least-squares equation in GraphPad Prism (version 4.0).

Synthesis of Aryl α-D-Galactosides. All aryl α-D-galactopyranosides, except the 3-nitrophenyl derivative, were synthesized from 1,2,3,4,6-penta-*O*-acetyl-D-galactopyranose using stannic chloride as the activator in CH_2Cl_2. Typically, 1,2,3,4,6-penta-*O*-acetyl-β-D-galactose (1.6 g, 4.0 mmol) and the appropriate phenol (1.5 g, 8 mmol) were dissolved in anhydrous CH_2Cl_2 (50 mL), and then $SnCl_4$ (0.8 mL, 8 mmol) was added. The reaction mixture was stirred at ambient temperature under an inert atmosphere for 48 h, at which time TLC analysis showed that the reaction was complete. Following the addition of water (35 mL), the reaction mixture was neutralized via addition of saturated $NaHCO_3$ (20 mL). The product was extracted from the aqueous layer using CH_2Cl_2 (3 × 35 mL), and the combined organic layer was washed with brine (2 × 20 mL), dried over Na_2SO_4, and then concentrated under reduced pressure to yield the crude product. This material was purified by column chromatography using an EtOAc/hexane mixture (1:4) as the eluent to yield the pure α-anomer. Deprotection was accomplished under Zemplen conditions using catalytic

dx.doi.org/10.1021/bi101808h |*Biochemistry* 2011, 50, 4298–4308

NaOMe in MeOH followed by neutralization of the solution with Amberlite (H^+) resin. Finally, product purification was achieved by crystallization from ethanol. The 3-nitrophenyl α-D-galactopyranoside was synthesized using $BF_3 \cdot OEt$ as the activator by following the reported reaction conditions.[13] The detailed characterizations of phenyl α-D-galactoside (**1a**) and 4-nitrophenyl α-D-galactoside (**2a**) have been previously reported.[14] The characterizations of all other unlabeled substrates used in this study are given below.

*3-Nitrophenyl α-D-galactoside (**2b**):* mp 165−168 °C; $[\alpha]^{20}_D$ = 195.7 (*c* = 0.15, H_2O); ^{1}H NMR (600 MHz, D_2O) δ 8.04 (s, 1 H, ArH), 8.00−7.97 (t, 1 H, ArH), 7.61−7.56 (m, 2 H, ArH), 5.79 (d, *J* = 3.8, 1 H, H-1), 4.12−4.01 (m, 4 H, H-2, H-3, H-4, H-5), 3.71 (app dd, *J* = 8.8, 6.2, 2 H, H-6, H-6′); ^{13}C NMR (151 MHz, D_2O) δ 156.42, 130.44, 124.03, 117.80, 112.04, 97.36, 72.02, 69.34, 69.05, 67.91, 60.95; ESI-MS for $C_{12}H_{15}NO_8$ *m*/*z* calcd for ($M + Na^+$) 324.0695, found 324.0682.

*3,4-Dichlorophenyl α-D-galactoside (**2c**):* mp 163−166 °C; ^{1}H NMR (400 MHz, D_2O) δ 7.50 (d, *J* = 8.9, 1 H, ArH), 7.40 (d, *J* = 2.8, 1 H, ArH), 7.11 (dd, *J* = 8.9, 2.8, 1 H, ArH), 5.66 (d, *J* = 3.7, 1 H, H-1), 4.10−3.96 (m, 4 H, H-2, H-3, H-4, H-5), 3.74−3.69 (m, 2 H, H-6, H-6′); ^{13}C NMR (126 MHz, D_2O) δ 155.32, 130.81, 125.37, 119.03, 117.12, 97.52, 71.83, 69.33, 69.04, 67.85, 60.91; ESI-MS for $C_{12}H_{14}Cl_2O_6$ *m*/*z* calcd for ($M + Na^+$) 347.0065, found 347.0054.

*3-Chlorophenyl α-D-galactoside (**2d**):* mp 139−142 °C; $[\alpha]^{20}_D$ = 195.7 (*c* = 0.499, H_2O); ^{1}H NMR (400 MHz, D_2O) δ 7.34 (t, *J* = 8.2, 1 H, ArH), 7.25 (t, *J* = 2.1, 1 H, ArH), 7.18−7.07 (m, 2 H, ArH), 5.67 (d, *J* = 3.9, 1 H, H-1), 4.11−3.93 (m, 4 H, H-2, H-3, H-4, H-5), 3.74−3.65 (m, 2 H, H-6, H-6′); ^{13}C NMR (126 MHz, D_2O) δ 156.78, 134.25, 130.69, 122.91, 117.47, 115.62, 97.28, 71.79, 69.35, 69.05, 67.95, 60.93; ESI-MS for $C_{12}H_{15}ClO_6$ *m*/*z* calcd for ($M + Na^+$) 313.0455, found 313.0441.

*4-Chlorophenyl α-D-galactoside (**2e**):* mp 157−161 °C; $[\alpha]^{20}_D$ = 193.5 (*c* = 0.452, H_2O); ^{1}H NMR (600 MHz, D_2O) δ 7.37 (d, *J* = 9.0, 2 H, ArH), 7.15 (d, *J* = 9.0, 2 H, ArH), 5.64 (d, *J* = 3.8, 1 H, H-1), 4.05−3.99 (m, 4 H, H-2, H-3, H-4, H-5), 3.70 (app d, *J* = 5.9, 2 H, H-6, H-6′), 3.34 (d, *J* = 1.0, OH); ^{13}C NMR (151 MHz, D_2O) δ 154.79, 129.45, 127.27, 118.72, 97.46 (C-1), 71.72, 69.36, 69.08, 67.98, 60.95; ESI-MS for $C_{12}H_{15}ClO_6$ *m*/*z* calcd for ($M + Na^+$) 313.0455, found 313.0445.

*4-Methylphenyl α-D-galactoside (**2f**):* mp 160−163 °C; $[\alpha]^{20}_D$ = 174.3 (*c* = 0.562, H_2O); ^{1}H NMR (500 MHz, D_2O) δ 7.22 (d, *J* = 8.4, 2 H, ArH), 7.08 (d, *J* = 8.5, 2 H, ArH), 5.60 (d, *J* = 3.9, 1 H, H-1), 4.13−4.03 (m, 3 H, H-3, H-4, H-5), 3.98 (dd, 1 H, H-2), 3.70 (app d, *J* = 5.7, 2 H, H-6, H-6′), δ 2.29 (s, 3 H, $ArCH_3$); ^{13}C NMR (126 MHz, D_2O) δ 153.92, 133.03, 130.13, 117.44, 97.65, 71.55, 69.40, 69.11, 68.05, 60.94, 19.55; ESI-MS for $C_{13}H_{18}O_6$ *m*/*z* calcd for ($M + Na^+$) 293.1001, found 293.0990.

Phenyl 2,3,4,6-Tetra-*O*-acetyl-α-D-[1-^{2}H]galactopyranoside (3b). 1,2,3,4,6-Penta-*O*-acetyl-D-[1-^{2}H]galactose (Supporting Information) (1.6 g, 4.0 mmol) and phenol (1.5 g, 8 mmol) were dissolved in anhydrous CH_2Cl_2 (50 mL) to which $SnCl_4$ (0.8 mL, 8 mmol) was added. This solution was stirred at room temperature for 48 h, at which time TLC analysis (40% EtOAc/hexane) showed that the reaction was complete. Following the addition of water (35 mL) and saturated $NaHCO_3$ (20 mL), the product was extracted from the aqueous layer using CH_2Cl_2 (3 × 35 mL). The combined organic layer was washed with brine and dried (Na_2SO_4). Removal of the volatiles under reduced pressure gave the crude product in quantitative yield. Flash chromatographic purification (25% EtOAc/hexane) gave 340 mg of the pure α-anomer **3a** and 600 mg of an anomeric mixture: $[\alpha]^{20}_D$ = 165.8 (*c* = 0.32, $CHCl_3$); ^{1}H NMR (400 MHz, $CDCl_3$) δ 7.34−7.27 (m, 2 H, Ar), 7.09−7.03 (m, 3 H, Ar), 5.58 (dd, 1 H, *J* = 10.8, 3.4, H-3), 5.53 (dd, 1 H, *J* = 3.4, 1.2, H-4), 5.28 (d, 1 H, *J* = 10.8, H-2), 4.38−4.33 (t, 1 H, H-5), 4.16−4.03 (m, 2 H, H-6, H-6′), 2.17, 2.07, 2.03, 1.94 (4s, 12 H, 4 × CH_3); ^{13}C NMR (151 MHz, solvent) δ 170.43, 170.33, 170.20, 170.06 (4 × C═O), 156.26 (Ar), 129.62 (Ar), 122.98 (Ar), 116.75 (Ar), 67.89 (C-4), 67.73 (C-2), 67.54 (C-3), 67.10 (C-5), 61.47 (C-6), 20.74, 20.69, 20.64, 20.57 (4 × CH_3); ESI-MS for $C_{20}H_{23}DO_{10}$ *m*/*z* calcd for ($M + Na^+$) 448.1330, found 448.1336.

Phenyl α-D-[1-^{2}H]Galactopyranoside (1b). Deprotection of **3b** under Zemplen conditions, using catalytic NaOMe in MeOH, was followed by neutralization using Amberlite (H^+) resin. The deprotected compound was further recrystallized from ethanol to yield 110 mg of **1b** (yield, 60%): mp 132−135 °C; $[\alpha]^{20}_D$ = 185.6 (*c* = 0.0.56, H_2O); ^{1}H NMR (400 MHz, D_2O) δ 7.47−7.36 (m, 2 H, Ar), 7.25−7.11 (m, 3 H, Ar), 4.16−4.05 (m, 3 H, H-3, H-4, H-5), 4.00 (d, 1 H, *J* = 10.1, H-2), 3.71 (app d, 2 H, *J* = 6.2, H-6, H-6′); ^{13}C NMR (151 MHz, D_2O) δ 129.82 (Ar), 123.07 (Ar), 117.34 (Ar), 71.60, 69.41, 69.12, 67.95, 60.95; ESI-MS for $C_{12}H_{15}DO_6$ *m*/*z* calcd for ($M + Na^+$) 280.0907, found 280.0904.

Phenyl 2,3,4,6-Tetra-*O*-acetyl-α-D-[2-^{2}H]galactopyranoside (3c). Dimeric 3,4,6-tri-*O*-acetyl-2-deoxy-2-nitroso-α-D-galactopyranosyl chloride **5**, made from galactal **4**,[15] was dissolved in anhydrous DMF (100 mL), and to this solution was added phenol (2 g, 2.0 equiv). The resultant mixture was stirred for 70 h at ambient temperature. At that time, TLC analysis (40% EtOAc/hexane) indicated the complete disappearance of the starting material. The reaction mixture was then diluted with Et_2O (50 mL) and extracted with water (3 × 40 mL), washed with brine (10 mL), dried (Na_2SO_4), and concentrated under reduced pressure to yield a yellow syrup. Purification by flash chromatography (35% EtOAc/hexane) gave phenyl 3,4,6-tri-*O*-acetyl-2-deoxy-2-oximino-α-D-*lyxo*-hexopyranoside **6** (1.3 g, 30% over two steps). The glycosylated product **6** (1.3 g) was dissolved in CH_3CN (15 mL) that contained 1 N HCl (0.5 mL) and CH_3CHO (0.2 mL). The reaction mixture was stirred at ambient temperature for 5 h, at which time the reaction mixture was extracted with EtOAc (3 × 25 mL). The combined organic layer was then dried (Na_2SO_4), and volatiles were removed under reduced pressure to give a pale yellow oil. The crude product was dissolved in anhydrous THF (30 mL); the solution was cooled to 0 °C, and a solution of $NaBD_4$ (100 mg) in cold D_2O (2 mL) was added. The mixture was then stirred at 0 °C for 1 h and then at room temperature for 2 h. Cautious addition of glacial AcOH (5 mL) destroyed the excess borodeuteride, and the resultant solution was washed with MeOH (20 mL). Removal of the volatiles under reduced pressure gave a pale yellow syrup that was directly acetylated under standard conditions, pyridine (5 mL) and Ac_2O (4 mL) at 25 °C. After the addition of water (30 mL), the product was extracted into CH_2Cl_2 (3 × 30 mL), and the organic layer was washed with cold 10% H_2SO_4 (10 mL) and brine (2 × 10 mL) and dried (Na_2SO_4). Removal of the volatiles under reduced pressure gave a pale yellow syrup that was purified by flash chromatography to give pure phenyl 2,3,4,6-tetra-*O*-acetyl-α-D-[2-^{2}H]galactopyranoside **3c** (350 mg, 30% over three steps): $[\alpha]^{20}_D$ = 168.3 (*c* = 0.247, $CHCl_3$); ^{1}H NMR (400 MHz, $CDCl_3$) δ 7.38−7.25 (m, 2 H, ArH), 7.14−7.03 (m, 3 H, ArH), 5.78 (s, 1 H, H-1), 5.58 (d, 1 H, *J* = 3.4, H-3), 5.53 (d, 1 H, *J* = 3.3, H-4),

4.36 (t, 1 H, J = 7.1, H-5), 4.09 (m, 1 H, H-6), 4.15 (m, 1 H, H-6′), 2.17, 2.08, 2.04, 1.94 (4s, 12 H, 4 × CH_3); ^{13}C NMR (151 MHz, $CDCl_3$) δ 170.42, 170.33, 170.21, 170.06, 156.26, 129.62 (Ar), 122.99 (Ar), 116.75 (Ar), 94.78 (C-1), 67.90 (C-4), 67.48 (C-3), 67.12 (C-5), 61.47 (C-6), 20.74, 20.68, 20.64, 20.56 (4 × CH_3, $COCH_3$); ESI-MS for $C_{20}H_{23}DO_{10}$ m/z calcd for (M + Na^+) 488.1330, found 448.1321.

Complete deprotection of the peracetylated compound was accomplished under Zemplen conditions using a NaOMe/MeOH mixture followed by neutralization using Amberlite (H^+) resin, to yield 175 mg (90%) of pure phenyl α-D-[2-^{2}H]galactopyranoside **1c**: mp 133−135 °C; $[\alpha]^{20}_D$ = 196.0; ^{1}H NMR (600 MHz, D_2O) δ 7.41 (dd, J = 8.3, 7.5, 2 H, ArH), 7.20 (d, J = 7.9, 2 H, ArH), 7.15 (s, 1 H, ArH), 5.68 (s, 1 H, H-1), 4.06−4.09 (m, 2 H, H-3, H-4), 4.06 (d, J = 3.3, 1 H, H-5), 3.70 (app d, J = 6.2, 2 H, H-6, H-6′); ^{13}C NMR (151 MHz, D_2O) δ 129.82 (Ar), 123.08 (Ar), 117.35 (Ar), 97.26 (C-1), 71.63 (C-5), 69.35 (C-3), 69.12 (C-4), 60.95 (C-6); ESI-MS for $C_{12}H_{15}DO_6$ m/z calcd for (M + Na^+) 280.0907, found 280.0905.

Dimeric 3,4,6-Tri-*O*-acetyl-2-deoxy-2-nitroso-α-D-[3-^{2}H]-galactopyranosyl Chloride (8). NOCl gas, which was prepared by dropwise addition of a saturated solution of sodium nitrite (13 g) in water (20 mL) to concentrated HCl (50 mL), was bubbled through a cooled solution (−45 °C) of thoroughly dried deuterated galactal **7** (Supporting Information) in EtOAc (40 mL). After the addition was complete, the sample was heated to 0 °C over a period of 20 min, and the volatiles were then removed under reduced pressure to give a bluish-green mass, which was further dried under vacuum for 2 h. The resultant crude product was used in the subsequent reaction without further purification.

Phenyl 2,3,4,6-Tetra-*O*-acetyl-α-D-[3-^{2}H]galactopyranoside (3d). The crude dimeric 3,4,6-tri-*O*-acetyl-2-deoxy-2-nitroso-α-D-[3-^{2}H]galactopyranosyl chloride **8** was dissolved in anhydrous DMF (50 mL), and to this solution was added phenol (800 mg, 2.0 equiv). Stirring was continued for 70 h at ambient temperature until TLC analysis (40% EtOAc/hexane) showed the presence of the desired product (R_f = 0.4). Subsequently, the reaction mixture was diluted with Et_2O (50 mL) and extracted with water (3 × 30 mL). The combined ethereal layers were pooled together, washed with brine (20 mL), dried over Na_2SO_4, and concentrated under vacuum to give a yellowish syrup that was purified by flash chromatography (35% EtOAc/hexane) to yield 330 mg (30% over two steps) of phenyl 3,4,6-tri-*O*-acetyl-2-deoxy-2-oximino-α-D-[3-^{2}H]-*lyxo*-hexopyranoside **9**. After **9** (330 mg) had been dissolved in CH_3CN (5 mL) containing 1 N HCl (0.5 mL) and CH_3CHO (0.3 mL), the mixture was stirred at ambient temperature for 5 h, when water (20 mL) was added. The aqueous layer was extracted with EtOAc (3 × 25 mL); the combined organic layer was dried (Na_2SO_4), and volatiles were then removed under reduced pressure to give a pale yellow oil. The resultant material was dissolved in anhydrous THF (30 mL), and the solution was cooled to 0 °C. Addition of a solution of $NaBH_4$ (100 mg) in cold H_2O (2 mL) was followed by the reaction being stirred at 0 °C for 1 h and then at room temperature for 2 h. Cautious addition of glacial AcOH (5 mL) destroyed the excess borohydride, and the resultant solution was washed with MeOH (20 mL). Removal of the volatiles under reduced pressure gave a pale yellow syrup that was directly acetylated under standard conditions, with stirring in pyridine (5 mL) and Ac_2O (4 mL) for 15 h at 25 °C. Flash chromatographic purification gave pure **3d** (80 mg, 40% yield over three steps): $[\alpha]^{20}_D$ = 167.0 (c = 0.15, $CHCl_3$); ^{1}H NMR (400 MHz, $CDCl_3$) δ 7.34−7.28 (m, 2 H, Ar), 7.09−7.03 (m, 3 H, Ar), 5.78 (d, 1 H, J = 3.6, H-1), 5.53 (d, 1 H, J = 1.1, H-4), 5.29 (d, 1 H, J = 3.7, H-2), 4.36 (t, 1 H, J = 6.6, H-5), 4.12 (dd, 1 H, J = 11.3, 6.2, H-6), 4.06 (dd, 1 H, J = 11.3, 7.1, H-6′), 2.17, 2.07, 2.03, 1.94 (4 × CH_3); ^{13}C NMR (151 MHz, $CDCl_3$) δ 170.41, 170.32, 170.20, 170.05 (4 × C═O, 4 × $OCOCH_3$), 156.28 (ArC), 129.62 (ArC), 122.99 (ArCH), 116.77 (ArCH), 94.84 (C-1), 67.86 (C-4), 67.74 (C-2), 67.13 (C-5), 61.47 (C-6), 20.73, 20.67, 20.63, 20.55 (4 × CH_3, 4 × $OCOCH_3$); ESI-MS for $C_{20}H_{23}DO_{10}$ m/z calcd for (M + Na^+) 488.1330, found 448.1330.

Complete deprotection of the peracetylated compound was accomplished under Zemplen conditions using a NaOMe/MeOH mixture followed by neutralization using Amberlite (H^+) resin, to yield pure phenyl α-D-[3-^{2}H]galactopyranoside **1d** in quantitative yield: mp 137−140 °C; $[\alpha]^{20}_D$ = 168.3 (c = 0.25, H_2O); ^{1}H NMR (600 MHz, D_2O) δ 7.46−7.38 (m, 2 H, Ar), 7.20 (d, J = 8.2, 2 H, Ar), 7.15 (t, J = 7.4, 1 H, Ar), 5.68 (d, J = 3.9, 1 H, H-1), 4.09 (t, J = 6.2, 1 H, H-5), 4.06 (s, 1 H, H-4), 3.99 (d, J = 3.9, 1 H, H-2), 3.70 (app d, J = 6.2, 2 H, H-6, H-6′); ^{13}C NMR (151 MHz, D_2O) δ 129.82 (Ar), 123.07 (Ar), 117.35 (Ar), 97.29 (C-1), 71.63 (C-5), 69.07 (C-4), 67.99 (C-2), 60.95 (C-6); ESI-MS for $C_{12}H_{15}DO_6$ m/z calcd for (M + Na^+) 280.0907, found 280.0900.

Phenyl 2,3,4,6-Tetra-*O*-acetyl-α-D-[2-^{2}H,3-^{2}H]galactopyranoside (3e). A solution of the ketone made from oxime **9** (285 mg, made as described above) in anhydrous THF (30 mL) was cooled to 0 °C, and then a solution of $NaBD_4$ (100 mg) in cold D_2O (2 mL) was added dropwise. After the reaction mixture had been stirred at 0 °C for 1 h and then at room temperature for 2 h, the cautious addition of glacial AcOH (5 mL) destroyed the excess borodeuteride. The resultant solution was washed with MeOH (20 mL), and removal of the volatiles under reduced pressure gave a pale yellow syrup, which was directly acetylated under standard conditions, pyridine (5 mL) and Ac_2O (5 mL) at 25 °C. The crude product was purified by flash chromatography (25% EtOAc/hexane) to yield pure peracetylated 2,3-dideuteriated compound **3e** (100 mg, 30% over two steps): ^{1}H NMR (400 MHz, $CDCl_3$) δ 7.38−7.24 (m, 2 H, Ar), 7.13−7.02 (m, 3 H, Ar), 5.78 (s, 1 H, H-1), 5.53 (d, 1 H, J = 1.0, H-4), 4.36 (t, 1 H, J = 6.5, H-5), 4.18−3.99 (m, 2 H, H-6, H-6′), 2.17, 2.05, 2.03, 1.94 (4 × CH_3); ^{13}C NMR (151 MHz, $CDCl_3$) δ 170.42, 170.33, 170.21, 170.06, 156.26, 129.62 (ArC), 122.99 (ArC) 116.75 (ArC), 94.78 (C-1), 67.86 (C-4), 67.12 (C-5), 61.47 (C-6), 20.74, 20.68, 20.64, 20.57 (4 × CH_3, $OCOCH_3$); ESI-MS for $C_{20}H_{22}D_2O_{10}$ m/z calcd for (M + Na^+) 449.1393, found 449.1371.

Final deprotection of the compound was accomplished under Zemplen conditions using a NaOMe/MeOH mixture followed by neutralization using Amberlite (H^+) resin and gave 40 mg (80%) of pure phenyl α-D-[2-^{2}H,3-^{2}H]galactopyranoside **1e**: mp 139−140 °C; $[\alpha]^{20}_D$ = 182.9; ^{1}H NMR (600 MHz, D_2O) δ 7.44−7.38 (m, 2 H, Ar), 7.20 (d, 2 H, J = 8.5, Ar), 7.18−7.11 (m, 1 H, Ar), 5.68 (s, 1 H, H-1), 4.08 (t, 1 H, J = 6.2, H-5), 4.05 (s, 1 H, H-4), 3.70 (d, 2 H, J = 6.3, H-6, H-6′); ^{13}C NMR (151 MHz, D_2O) δ 156.09 (Ar), 129.82 (Ar), 123.07 (Ar), 117.34 (Ar), 97.26 (C-1), 71.63 (C-5), 69.07 (C-4), 60.94 (C-6); ESI-MS for $C_{12}H_{14}D_2O_6$ m/z calcd for (M + Na^+) 281.0970, found 281.0966.

Cloning of α-Galactosidase. The *MelA* gene encoding α-galactosidase was PCR amplified from *C. freundii* genomic DNA (ATCC 8090D). The amplification was performed in 5%

DMSO using the following primers that introduced NheI and XhoI restriction sites (underlined) into the forward and reverse primers, respectively: 5′-CGCGGCTAGCATGATGTCTG-CACCC-3′ (forward) and 5′-GCGCCTCGAGTTAACGGTG-CAGCCAG-3′ (reverse). The PCR fragment was purified, digested with NheI and XhoI, inserted into the correspondingly digested pET28a vector (Novagen), and transformed in *E. coli* BL-21(DE3). The plasmid DNA was isolated from a single colony and verified by restriction digestion and DNA sequencing by Macrogen using T7 promoter and T7 terminator primers.

MelA Expression and Purification. For expression of the *MelA* gene, cells were inoculated in Luria broth and then expressed in YT medium supplemented with 1% kanamycin at 37 °C to an OD_{600} of 0.5 before being induced with 0.5 mM IPTG. The cultures were incubated at 25 °C for 5 h and then centrifuged (10 min at 8400*g*), and the pellet from 1 L of culture was resuspended in binding buffer containing 5 mM imidazole. The cells were lysed open using 1% lysozyme (from chicken egg white) and a protease inhibitor cocktail tablet followed by sonication (20 s on−40 s off cycle at 60% capacity) to ensure complete lysis of the cells. The lysate was centrifuged at 4 °C (34000*g*) to remove the cell debris and intact cells. The clear supernatant was collected and filtered through a 0.45 μm filter before being loaded on to a HiTrap Chelating HP column (5 mL) that had been pre-equilibrated with binding buffer. The column was washed sequentially with 60, 100, and 150 mM imidazole before the protein was eluted with 250 mM imidazole. Fractions containing pure His-*MelA*, as determined by 10% sodium dodecyl sulfate−polyacrylamide gel electrophoresis, were pooled together and dialyzed, at 4 °C, three times against 4 L of Tris buffer (20 mM, pH 7.0) that contained NaCl (100 mM) and DTT (6 mM). The protein was then concentrated by centrifugation through a 10 kDa filter, and its concentration was determined (Bradford Assay or Nanodrop).

Enzyme Kinetics. All kinetic assays were conducted in either 0.2 or 1.0 cm path length quartz cuvettes, unless stated otherwise, using a Cary 300 UV−vis spectrometer equipped with a Cary temperature controller. For all experiments, the MelA α-galactosidase was preincubated in assay buffer with cofactors at 37 °C for 15 min prior to the addition of the substrate, which initiated the enzymatic reaction. The following buffer (buffer A) at pH 7.5 was used for most kinetic experiments: HEPES (50 mM), $MnCl_2$ (1.0 mM), NAD^+ (100 μM), 2-mercaptoethanol (10 mM), and BSA (0.1%, w/v). All cofactor solutions were freshly prepared before each set of kinetic assays. The measurements of all deuterium kinetic isotope effects were performed in buffer B, which was identical to buffer A except that the added reducing agent was TCEP (1 mM) instead of 2-mercaptoethanol (10 mM).

Typical Conditions for the Measurement of Michaelis−Menten Parameters. The concentration of α-galactosidase was chosen such that less than 10% of the total substrate was consumed during the assay. For each assay, the enzyme was incubated in the appropriate buffer at 37 °C for either 15 or 20 min. Afterward, the reaction was initiated by the addition of substrate. The initial rate of hydrolysis was followed spectrophotometrically at the wavelength of the maximal absorbance change. Typically, the substrate concentration was varied between 40 μM and 1 mM, and the measured initial rate versus concentration data were fit to a standard Michaelis−Menten equation.

Determination of the pH−Rate Profile. To determine the effect of pH on enzymatic activity, we measured kinetic parameters over a pH range of 4.0−9.5. The following buffers were used: NaOAc-HOAc (20 mM, pH 4.0−4.5), MES (20 mM, MES-NaOH, pH 6.0−6.7), HEPES (20 mM, pH 6.5−8.2), and CHES (20 mM, pH 8.5−9.5). Typical assay conditions were as follows. α-Galactosidase (final concentration of 4.1 μg/mL) was incubated at 37 °C with the appropriate buffer containing NaCl (50 mM), $MnCl_2$ (1.0 mM), NAD^+ (100 μM), 2-mercaptoethanol (10 mM), and BSA (0.1%, w/v) for 10 min prior to the addition of substrate 4NPαG; the hydrolysis reaction was monitored at either 400 nm (pH 6.5−9.0) or 340 nm (pH 4.0−6.0). The difference in the extinction coefficients ($\Delta\varepsilon$) for 4NPαG and the released phenolate/phenol was determined at each pH, and the initial rate measurements were fit to a standard Michaelis−Menten equation.

Kinetic Investigation of NAD^+ Cofactor Dependence. A sample of MelA (final concentration of 16.3 μg/mL) in buffer A was preincubated for 15 min at 37 °C for 15 min. 4NPαG was added to the solution to initiate the hydrolysis reaction. In another parallel assay, the enzyme was incubated with all other cofactors at pH 7.5 in the presence of 10 mM $NaBH_4$, for the quantitative reduction of NAD^+ to NADH. The enzyme was completely inactive after treatment with $NaBH_4$, but approximately 60% of its activity was restored upon addition of exogenous NAD^+ (200 μM).

Determination of K_d Values for NAD^+. Solutions containing MelA (final concentration of 15.8 μg/mL) and NAD^+ (concentration varied from 20 μM to 4 mM) were preincubated in HEPES buffer (50 mM, pH 7.5) containing $MnCl_2$ (1 mM), 2-mercaptoethanol (10 mM), and BSA (0.1%, w/v) at 37 °C for 15 min, and then 4NPαG (final concentration of 100 μM) was added to initiate the reaction (final volume of 400 μL). The measured initial reaction rates were fit to the Michaelis−Menten equation that includes a term for substrate inhibition.

Determination of the K_d Value for Mn^{2+}. To remove bound metal ions, MelA was dialyzed three times against 4 L of Tris buffer (20 mM, pH 7.1). Solutions containing MelA (final concentration of 15.0 μg/mL) and Mn^{2+} (concentration varied from 0 to 400 μM) were preincubated in HEPES buffer (50 mM, pH 7.5) containing NAD^+ (100 μM), 2-mercaptoethanol (10 mM), and BSA (0.1%, w/v) at 37 °C for 15 min, and then 4NPαG (final concentration of 100 μM) was added to initiate the reaction (final volume of 400 μL). In a separate experiment, a solution of MelA (200 μL, 3 mg/mL) was dialyzed overnight against Tris-HCl buffer (500 mL, 20 mM, pH 7.1) containing EDTA (2 mM) and NaCl (100 mM). The resultant enzyme solution was then dialyzed twice, for 4 h, against fresh Tris-HCl buffer (500 mL, 20 mM, pH 7.1) containing NaCl (100 mM). The enzyme activity was then monitored as a function of Mn^{2+} concentration as detailed above. After subtraction of the rate in the absence of Mn^{2+}, the resultant initial rates were fit to a standard Michaelis−Menten equation.

Deuterium Kinetic Isotope Effect Measurements. To determine KIEs (k_H/k_D) on *V*, separate measurements of the Michaelis−Menten parameters were taken for each of the following: phenyl α-D-galactopyranoside, phenyl α-D-[1-^{2}H]galactopyranoside, phenyl α-D-[2-^{2}H]galactopyranoside, phenyl α-D-[3-^{2}H]galactopyranoside, and phenyl α-D-[2-^{2}H,3-^{2}H]galactopyranoside. Typically, for each assay, MelA α-galactosidase (final concentration of 3.1 μg/mL) was incubated in buffer B for 20 min prior to the initiation of hydrolysis by the addition of substrate. The initial rates were measured by monitoring the release of phenol at 270 nm. The substrate concentration was varied between 0.04 and 1.0 mM. The cofactor solution was prepared freshly, and all the data sets were

obtained using the same stock of cofactors and enzyme. Each set of kinetic experiments was completed within a day to ensure the smallest possible variation in enzyme activity. All kinetic data were fit to a standard Michaelis−Menten equation.

Conditions for the Measurement of KIEs on *V/K*. Measurements of individual V/K values were taken by monitoring the first-order consumption of substrate, whose concentration was typically $\leq 0.1K_m$, at the wavelength of the maximal absorbance change (277 nm). Normally, MelA α-galactosidase (final concentration in the range of 40−50 μg/mL) was incubated in buffer B for 20 min at 37 °C before addition of the appropriate substrate that initiated the reaction. The absorbance was monitored at 277 nm until the hydrolysis was complete. The absorbance versus time data were fit to a standard first-order rate equation; for all cases, it was determined that the fitting residuals were randomly scattered around zero. Measurements for the protio and deuterio substrates were performed in an alternating fashion, and each measurement was repeated three times. The resulting $^{D}V/K$ values were calculated using a standard weighted average method.[16]

Product Studies. ^{1}H NMR spectroscopy (500 MHz) was employed to identify the stereochemical course of the enzyme-catalyzed reaction. The reaction conditions involved incubating, at 37 °C, the enzyme (4.2 μg/mL) in buffer A containing CD_3OD (5 M). After the addition of 4NPαG (2.5 mg), the reaction was allowed to proceed at 37 °C until TLC analysis [1:4 (v/v) MeOH:EtOAc] showed no remaining starting material. Removal of the enzyme by centrifugal ultrafiltration at 4 °C was followed by stirring of the resultant solution with Chelex resin (Fluka) for 60 min. Following filtration, the solution was lyophilized and the resulting solid was dissolved in D_2O, and then the ^{1}H NMR spectrum was recorded.

Brønsted Analysis of the Linear Free Energy Relationship. A series of substrates with varying leaving groups were synthesized to perform a Brønsted analysis. Full Michaelis−Menten curves were measured, in buffer A, for each substrate using the protocol listed above.

RESULTS

To test whether *C. freundii* MelA galactosidase displays any catalytic reactivity toward phosphorylated substrates, 4-nitrophenyl 6-phospho-α-D-galactoside was synthesized (Supporting Information). However, it was shown that MelA hydrolyzed neither 4-nitrophenyl 6-phospho-α-D-galactopyranoside nor 4-nitrophenyl β-D-galactopyranoside, while it was catalytically active against 4-nitrophenyl α-D-galactopyranoside (data not shown). The absolute requirement for the catalytic activity of this GH4 α-galactosidase for NAD^+ was shown by a standard borohydride reduction experiment (Figure S1 of the Supporting Information). The binding constants for the two cofactors, NAD^+ and Mn^{2+}, were determined by monitoring the hydrolysis of 4NPαG as a function of cofactor concentration at pH 7.5 and 37 °C. The dependence of enzyme activity on the concentration of NAD^+ exhibited marked substrate inhibition (Figure 1), and the associated kinetic parameters for the MelA α-galactosidase-catalyzed reaction (K_m and K_{is}) are 240 ± 40 μM and 2.0 ± 0.4 mM, respectively. In the absence of Mn^{2+}, the enzyme exhibited an activity that was approximately 10% of its maximal value, and after subtraction of this residual activity from the initial rates measured in the presence of Mn^{2+}, an estimate of 220 ± 100 μM was made for the binding constant of Mn^{2+} (K_d) (Figure S2 of the Supporting Information). All other kinetic parameters were evaluated using buffers that contained NAD^+ and Mn^{2+} at concentrations of 100 μM and 1.0 mM, respectively.

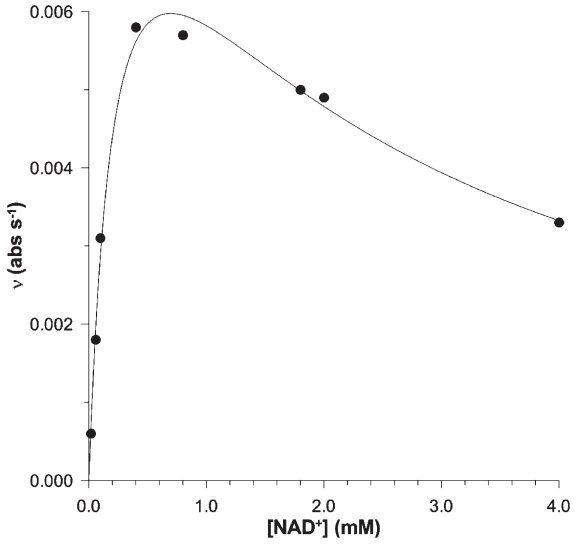

Figure 1. Ligand binding curve for NAD^+ using PNPαG as the substrate.

Table 1. Michaelis−Menten Kinetic Parameters for the MelA-Catalyzed Hydrolysis of 4NPαG as a Function of pH at 37 °C

pH	k_{cat} (s^{-1})	$10^{-3} \times k_{cat}/K_m$ (M^{-1} s^{-1})
4.5	0.12 ± 0.05	0.091 ± 0.070
6.7	0.30 ± 0.04	0.81 ± 0.26
7.1	1.05 ± 0.05	2.7 ± 0.4
7.5	1.68 ± 0.11	5.8 ± 1.1
7.8	2.07 ± 0.21	9.9 ± 1.9
8.0	1.75 ± 0.08	8.9 ± 1.4
8.4	1.37 ± 0.03	15.6 ± 1.5
8.7	0.62 ± 0.03	5.0 ± 1.2
9.0	0.23 ± 0.03	0.96 ± 0.42

Product Studies. In the absence of a reducing agent, MelA gave no product even after incubation for 48 h, and when the reaction was performed with mercaptoethanol in the presence of methanol (5 M), no methyl galactoside was produced. However, an additional new anomeric resonance, in addition to galactose, appeared in the ^{1}H NMR spectrum at a chemical shift of δ 5.8 ($J_{1,2}$ = 5.5 Hz) that is tentatively assigned to an α-galactoside.

The variations in kinetic parameters k_{cat}/K_m and k_{cat} for the enzyme-catalyzed hydrolysis of 4-nitrophenyl α-D-galactopyranoside as a function of pH are listed in Table 1. The kinetic data for k_{cat} were fit to a classic bell-shaped pH−rate curve (Figure 2); however, the resultant calculated pK_a values, for the two catalytically important ionizations, were not well-resolved, with both values being 7.8 ± 0.5. In addition, the gross shape of the pH−rate curve on k_{cat}/K_m is similar, with the maximal activity occurring at pH ~8.0 (Figure S3 of the Supporting Information), but the fit of the kinetic data to a standard bell-shaped profile is particularly ill-defined.

dx.doi.org/10.1021/bi101808h |*Biochemistry* 2011, 50, 4298–4308

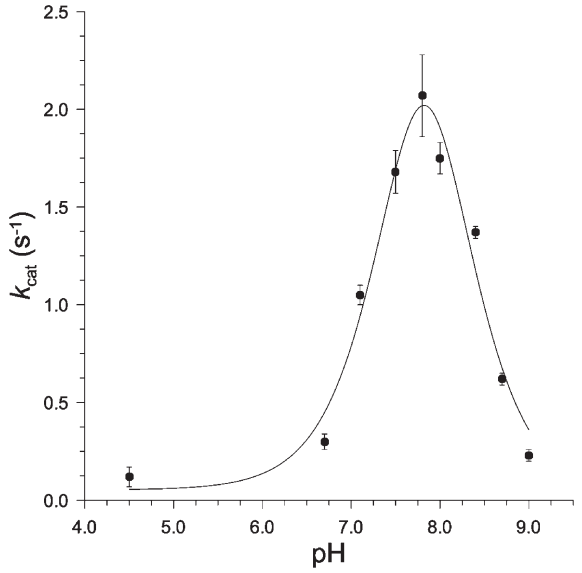

Figure 2. pH dependence of k_{cat} for the MelA-catalyzed hydrolysis of 4NPαG.

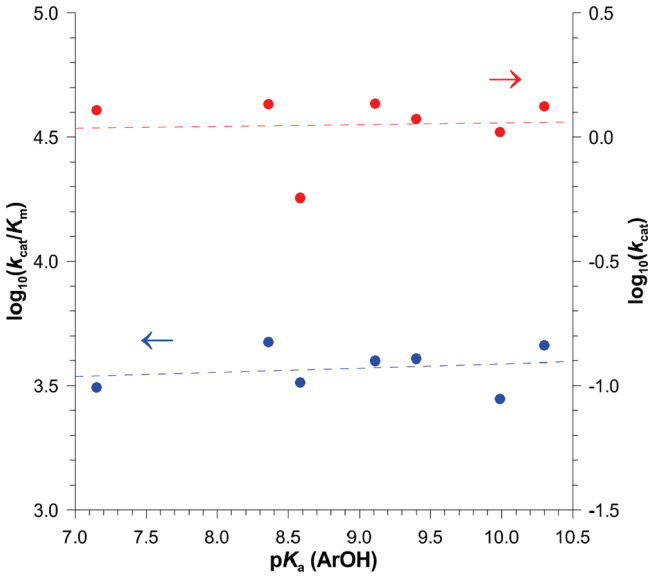

Figure 3. Brønsted plots for MelA-catalyzed hydrolysis, measured at 37 °C, of a series of aryl α-galactopyranosides and the associated pK_a values for the leaving group phenol. Colored red and blue are the k_{cat} and k_{cat}/K_m kinetic data, respectively.

A panel of seven aryl α-D-galactosides was synthesized by following literature procedures using peracetylated galactose as the starting material (see Materials and Methods for details). Full Michaelis−Menten curves were measured at pH 7.5 for each substrate (Table S1 of the Supporting Information), and the associated Brønsted β_{lg} values on k_{cat} and k_{cat}/K_m are −0.01 ± 0.02 and 0.02 ± 0.04, respectively (Figure 3).

Synthesis of Deuterated Substrates. Phenyl α-D-[1-^{2}H]-galactopyranoside was made using peracetylated [1-^{2}H]galactose (Supporting Information) as the starting material. All other deuterated phenyl α-D-galactopyranosides were made by the appropriate choice of reducing agent and starting tri-*O*-acetal D-galactal (**4** or **7**, 3,4,6-tri-*O*-acetyl-1,5-anhydro-2-deoxy-D-*lyxo*-hex-1-enitol) using the nitrosyl chloride addition reaction (Scheme 2) pioneered by Lemieux and co-workers.[17] Deuterated **7** was made by reduction of a known 3-keto compound[18] using sodium borodeuteride in place of borohydride[19] followed by a standard acetylation reaction (Supporting Information).

Deuterium Kinetic Isotope Effects. To measure KIEs on V/K, we used the substrate depletion method (Materials and Methods). Of note, in these experiments, TCEP was used as the reducing agent because in the presence of 2-mercaptoethanol the background absorbance at 277 nm exhibited a slow increase over time, a phenomenon that was traced to the reducing agent, and this resulted in large errors for the measured rate constants. In addition, to determine if the measured deuterium KIEs for H-2 and H-3 report on two sequential reactions that involve cleavage of a C−H bond, namely, (i) the transfer of a hydride to NAD^+ during oxidation of the 3-OH group and (ii) base-catalyzed removal of the C-2 proton, or if they originate from a single transition state, $^DV/K$ effects on deuterated substrates were measured using the dideuterated substrate phenyl α-D-[2-^{2}H,3-^{2}H]galactopyranoside. For the sake of consistency, KIEs on V_{max} were also measured with TCEP as the reducing agent. In these experiments, full Michaelis−Menten kinetic profiles were measured and the resultant V_{max} values were used to determine the ^DV effects. Tables 2 and 3 list the calculated KIEs for the MelA-catalyzed hydrolysis of PαG.

DISCUSSION

The *MelA* gene from *E. coli*, which was proposed to encode a GH4 α-galactosidase, has previously been cloned and sequenced.[11] The sequence data showed that the *MelA* gene encodes a 450 amino acid-protein that has a predicted molecular mass of 50.6 kDa.[11] In this work, the *MelA* gene from *C. freundii* was cloned and recombinantly expressed in *E. coli* so a detailed mechanistic study of this GH4 glycosidase could be performed. As with other family 4 glycosyl hydrolases,[6,9,10] the MelA enzyme from *C. freundii* requires two cofactors, NAD^+ and Mn^{2+}, as well as reducing conditions for maximal activity. Moreover, this α-galactosidase is incapable of hydrolyzing 4-nitrophenyl 6-phospho-α-D-galactopyranoside. Anggraeni et al. showed that for natural substrates the rMel4A α-galactosidase from *Bacillus halodurans* displays higher rates of turnover and catalytic efficiencies (k_{cat} and k_{cat}/K_m, respectively) for the disaccharide melibiose [α-D-Gal*p*-(1→6)-D-Glc*p*] than for the trisaccharide raffinose [α-D-Gal*p*-(1→6)-α-D-Glc*p*-(1↔2)β-D-Fru*f*].[12]

The dependence of the catalytic activity of *C. freundii* MelA α-galactosidase on the presence of NAD^+ was shown by incubating the enzyme with NAD^+ in the presence of $NaBH_4$ (10 mM), conditions under which NAD^+ is reduced to NADH. The *C. freundii* α-galactosidase was completely inactive under these conditions, but after addition of a solution of NAD^+ (200 μM) to the reaction medium, approximately 60% of the initial enzyme activity was restored (Figure S1 of the Supporting Information). Furthermore, the catalytic activity of the MelA α-galactosidase varied as a function of NAD^+ concentration, and the activity profile is consistent with the occurrence of substrate inhibition [K_d = 240 ± 40 μM, and K_{is} = 2.0 ± 0.4 mM (Figure 1)]. As a result, we decided to measure enzyme kinetic parameters at subsaturating concentrations of NAD^+. The variation in enzyme activity as a function of Mn^{2+} concentration showed no evidence of substrate inhibition, and all further kinetic experiments were performed at saturating Mn^{2+} levels (1.0 mM; $K_d \approx 0.2$ mM).

Scheme 2. Synthetic Reactions Used in the Synthesis of C-2- and C-3-Deuterated PαG Substrates

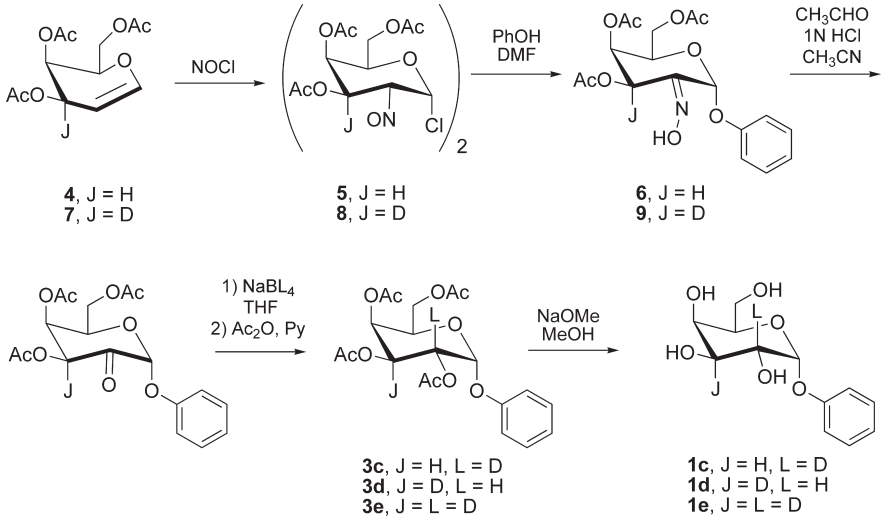

Table 2. Kinetic Isotope Effects on V/K for the MelA α-Galactosidase-Catalyzed Hydrolysis of Phenyl α-D-Galactopyranoside at pH 7.5 and 37 °C

isotopologue 1	isotopologue 2	$^{D}V/K^{a}$
PαG	[1-^{2}H]PαG	1.13 ± 0.07
PαG	[2-^{2}H]PαG	1.74 ± 0.06
PαG	[3-^{2}H]PαG	1.74 ± 0.05
[3-^{2}H]PαG	[2,3-^{2}H$_2$]PαG	1.71 ± 0.12
[2-^{2}H]PαG	[2,3-^{2}H$_2$]PαG	1.71 ± 0.13

[a] V/K(isotopologue 1)/V/K(isotopologue 2) ratio.

Table 3. Kinetic Isotope Effects on V for the MelA α-Galactosidase-Catalyzed Hydrolysis of Deuterated Phenyl α-D-Galactopyranoside at pH 7.5 and 37 °C

isotopologue 1	isotopologue 2	$^{D}V^{a}$
PαG	[1-^{2}H]PαG	1.06 ± 0.07
PαG	[2-^{2}H]PαG	0.91 ± 0.04[b]
PαG	[3-^{2}H]PαG	1.02 ± 0.06
[3-^{2}H]PαG	[2,3-^{2}H$_2$]PαG	0.91 ± 0.06[c]
[2-^{2}H]PαG	[2,3-^{2}H$_2$]PαG	1.01 ± 0.06

[a] V_{max}(isotopologue 1)/V_{max}(isotopologue 2) ratio. [b] Repeat measurement gave a value of 0.99 ± 0.08. [c] Repeat measurement gave a value of 0.98 ± 0.08.

Anggraeni et al. showed, for the Mel4a GH4 α-galactosidase from *B. halodurans*, that in the presence of reducing agent DTT both Co^{2+} and Fe^{2+} also gave active enzyme.[12] In contrast to the reported results with the 6-phosphoglucosidases *GlvA* and *BglT*,[6,9] which are also members of glycosyl hydrolase family 4 (GH4), no activity was observed with MelA in the absence of reducing agents. Also, when MelA-catalyzed hydrolysis of 4NPαG was performed in the presence of methanol (5 M), no trapping by methanol was observed. Consequently, the stereochemical outcome of MelA α-galactosidase-catalyzed reactions was inferred, by analogy to other previously characterized GH4 hydrolases, to be a retaining enzyme. Also of note, when the MelA-catalyzed hydrolysis 4NPαG was performed in D_2O, the reaction product, galactose, was completely deuterated at C-2 as shown by the ^{1}H NMR spectrum in which the anomeric protons for both anomers were singlets.

A detailed pH−rate profile for the catalyzed hydrolysis of 4NPαG was measured, and the kinetic data were fit to a standard bell-shaped curve where the pK_a values for the two catalytically important groups are approximately 7.8−8.0 (Figure 2 and Figure S3 of the Supporting Information).

To probe the effects of leaving group ability on catalytic activity, we synthesized a panel of seven aryl α-D-galactopyranoside substrates (structures **1a** and **2a**−**f**). The derived Brønsted β_{lg} values, for these substrates in which the pK_a of the conjugate acid of the aglycone varied by more than 3 pK_a units, on both k_{cat} and k_{cat}/K_m are, within experimental error, indistinguishable from zero (Figure 3). Therefore, it can be concluded that cleavage of the anomeric C−O bond is not kinetically significant for the MelA α-galactosidase-catalyzed hydrolysis of aryl α-D-galactopyranosides.

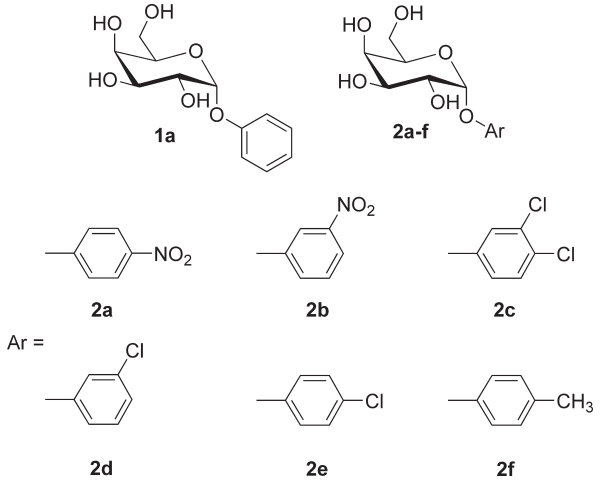

Withers and co-workers have also concluded that glycosidic bond cleavage was not a kinetically important event for either the

dx.doi.org/10.1021/bi101808h |*Biochemistry* 2011, 50, 4298–4308

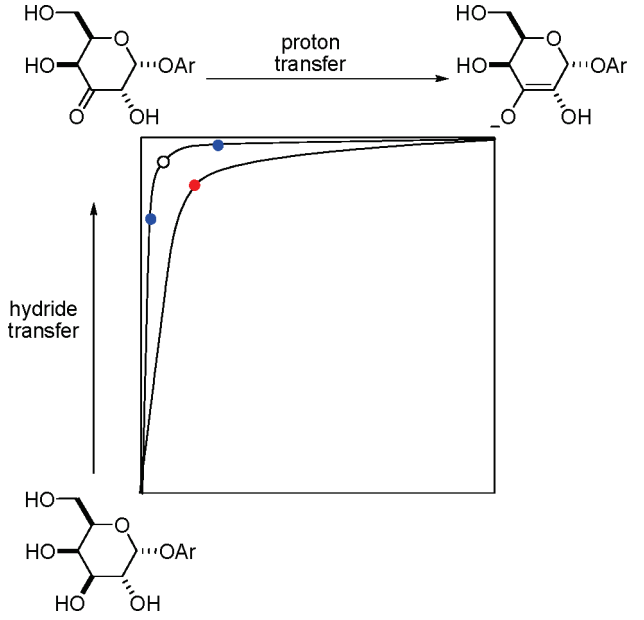

Figure 4. More O'Ferrall−Jencks diagram showing the possible transition state (red circle) for the concerted reaction from the Michaelis complex to the enediol intermediate that circumvents formation of the bound ketone (○). Also shown are plausible transition states (blue circles) for the previously proposed stepwise mechanism.[6,9] The enzymatic cofactors, NAD^+ and Mn^{2+}, have been omitted from the diagram for the sake of clarity.

T. maritima BglT 6-phospho-β-glucosidase[6] or the *B. subtilis* GlvA 6-phospho-α-glucosidase[9] GH4 enzyme. A detailed KIE study was undertaken to delineate the important transition states for the MelA enzyme-catalyzed reaction. That is, several different isotopologues that possessed a weakly activated leaving group were synthesized (Scheme 2 and the Supporting Information). Listed in Tables 2 and 3 are the measured V/K and V KIE values for deuteration at C-1, C-2, or C-3. Of note, the tabulated ^{D}V and $^{D}V/K$ values are markedly different. At first glance, the magnitudes of the $^{D}V/K$ effects measured at both the C-2 (1.74 ± 0.06) and C-3 (1.74 ± 0.05) centers suggest that both oxidation and proton abstraction are kinetically significant in accordance with previously reported conclusions.[6,9] To verify this analysis, we decided to measure the isotope effects associated with deuterated substrates. That is, if the C-2 and C-3 KIEs arise from a virtual transition state resulting from two sequential steps, we would expect that the KIE on C-2 should decrease if both isotopologues (C-2-H and C-2-D) are deuterated at C-3. In other words, if deuteration at C-3 increases the kinetic barrier for hydride transfer, then, for a stepwise mechanism, the magnitude of the ^{2}H KIE from deuteration at C-2 must decrease for the C-3-deuterated substrates relative to that measured with the C-3 nondeuterated galactosides;[20] i.e., $^{D}V/K$(C-2) > $^{D}V/K$(C-2,3-^{2}H).

Therefore, phenyl α-D-[2-^{2}H,3-^{2}H]galactoside was synthesized (Scheme 2), and both the $^{D}V/K$(C-2,3-^{2}H) and $^{D}V/K$(C-3,2-^{2}H) KIEs were measured (Table 2). Of note, neither $^{D}V/K$(C-2) nor $^{D}V/K$(C-3) shows any significant decrease in magnitude upon incorporation of a remote deuterium (Table 2).

An estimate of the expected reduction in $^{D}V/K$ values upon incorporation of a second deuterium can be made by deriving the kinetic expressions for Scheme 1, in which oxidation (k_3) and proton abstraction (k_5) are separate kinetic events. Thus, the formula for $^{D}V/K$(C-3) is given in eq 1

$$^{D}\left(\frac{V}{K_{C\text{-}3}}\right)_{C\text{-}2\text{-}H} = \frac{^{D}k_3 + \frac{k_{3H}}{k_2} + \frac{k_{4H}}{k_{5H}}\left(1 + \frac{k_{6H}}{k_7}\right)^{D}K_{eq}}{1 + \frac{k_{3H}}{k_2} + \frac{k_{4H}}{k_{5H}}\left(1 + \frac{k_{6H}}{k_7}\right)} \quad (1)$$

where $^{D}k_3$ is the intrinsic isotope effect on k_3 and $^{D}K_{eq}$ is the equilibrium isotope effect (EIE) on this step. The ratios of individual kinetic terms in eq 1 are normally termed commitment factors, either forward or reverse;[21] i.e., $c_f = k_{3H}/k_2$, and $c_r = k_{4H}/k_{5H}(1 + k_{6H}/k_7)$. However, to prevent confusion with different commitment factors for the oxidation and proton removal steps, we used the individual kinetic terms in the equations.

The corresponding expression for $^{D}V/K$(C-2) is given in eq 2 (Scheme 1). Given the kinetic insignificance of aglycone departure as shown by the β_{lg} value of zero (k_7, Scheme 1), the term k_{6H}/k_7 must be small ($k_7 \gg k_{6H}$).

$$^{D}\left(\frac{V}{K_{C\text{-}2}}\right)_{C\text{-}3\text{-}H} = \frac{^{D}k_5 + \frac{k_{5H}}{k_{4H}}\left(1 + \frac{k_{3H}}{k_2}\right) + \frac{k_{6H}}{k_7}{}^{D}K_{eq}}{1 + \frac{k_{5H}}{k_{4H}}\left(1 + \frac{k_{3H}}{k_2}\right) + \frac{k_{6H}}{k_7}} \quad (2)$$

Equation 3 can be derived for the expected V/K KIE on C-3 when C-2 is deuterated, if $k_{6H}/k_7 \approx 0$ (Supporting Information).

$$^{D}\left(\frac{V}{K_{C\text{-}3}}\right)_{C\text{-}2\text{-}D} = \frac{^{D}K_{eq}\left[^{D}\left(\frac{V}{K_{C\text{-}2}}\right)_{C\text{-}3\text{-}H} - 1\right] + {}^{D}\left(\frac{V}{K_{C\text{-}3}}\right)_{C\text{-}2\text{-}H}}{^{D}\left(\frac{V}{K_{C\text{-}2}}\right)_{C\text{-}3\text{-}H}} \quad (3)$$

Using the measured $^{D}V/K$(C-2) and $^{D}V/K$(C-3) values (both equal 1.74) in conjunction with the reported EIE ($^{D}K_{eq}$ = 1.18) for oxidation of cyclohexanol by NAD^+,[22] the estimated value for the magnitude of the $^{D}V/K$(C-3,2-^{2}H) effect is 1.50 (Supporting Information). Of note, the incorporation of a second deuterium at C-2 also results in a secondary equilibrium isotope effect for the hydride transfer reaction (kinetic terms k_{3H} and k_{4H}), and this (K_H/K_D) is expected to be approximately 1.054.[22] Incorporation of this value into eq 3, which results in modification of the value of $^{D}K_{eq}$ to 1.24 (1.18 × 1.054), gives an expected effect for $^{D}V/K$(C-3,2-^{2}H) of 1.53 (Supporting Information).

A similar formula (eq 4; see the Supporting Information) can be derived for the value of $^{D}V/K$(C-2,3-^{2}H). Coincidentally, the expected value for $^{D}V/K$(C-2,3-^{2}H), based on eq 4, is either 1.50 or 1.53 depending on whether the secondary EIE correction noted above is included in the calculations.

$$^{D}\left(\frac{V}{K_{C\text{-}2}}\right)_{C\text{-}3\text{-}D} = \frac{^{D}\left[\left(\frac{V}{K_{C\text{-}2}}\right)_{C\text{-}3\text{-}H} - 1\right]{}^{D}K_{eq}}{^{D}\left(\frac{V}{K_{C\text{-}3}}\right)_{C\text{-}2\text{-}H}} + 1 \quad (4)$$

Of note in the current example, the calculated values for both $^{D}V/K$(C-3,2-^{2}H) and $^{D}V/K$(C-2,3-^{2}H) are independent of the intrinsic KIEs ($^{D}k_3$ and $^{D}k_5$) or any commitment factors. Of note, given the standard error associated with the measured

dx.doi.org/10.1021/bi101808h |*Biochemistry* 2011, 50, 4298–4308

value for $^{D}V/K$(C-2,3-^{2}H) of 0.12 (Table 1), there is either a 4% likelihood, i.e., 100% − 50% (value of >1.74) − 46% (value between 0 and 1.75 standard deviations below 1.71), that the data are consistent with the stepwise mechanism or a 6.7% probability when the EIE value is included in the calculations. Thus, the measured $^{D}V/K$ values on dideuterated substrates of 1.71 (Table 1) are more consistent with a concerted reaction for oxidation and proton removal.

A single concerted step requires that abstraction of the C-2 proton by the active site base start prior to completion of C-3 oxidation by the transfer of a hydride to the on-board NAD^+ cofactor (Figure 4). In other words, during oxidation at C-3 to form the ketone the C-2 proton becomes progressively more acidic by virtue of the increasing polarization at C-3 and the proximal Mn^{2+} ion until transfer begins, which in this case results in the circumvention of formation of the proposed ketone intermediate (Figure 4).

The magnitudes of the $^{D}V/K$ values (on C-2 and C-3) reported here for the MelA reactions of phenyl α-galactopyranoside are similar to, albeit a little larger than, those reported for the *B. subtilis* GlvA-catalyzed hydrolysis of 4-nitrophenyl 6-phospho-α-glucopyranoside,[9] a result that implies GH4 enzymatic reactions that involve trans elimination reactions may proceed through very similar transition state structures. In this study, the negligible β_{lg} values notwithstanding, no information about the mechanism for the trans elimination reaction is available, a situation that contrasts the cis eliminations encountered with GH4 β-glycosidase where the $^{D}V/K$ values on C-2 are significantly higher than those reported here.[6,10]

The large relative errors associated with the normal secondary deuterium KIE at the anomeric center, $^{D}V/K$(C-1), make a detailed discussion of the origin of the effect difficult at present, although the minimal Brønsted β_{lg} values are inconsistent with the occurrence of any TS rehybridization at this position.

The measured KIEs on V for the MelA α-galactosidase-catalyzed hydrolysis of phenyl α-galactoside are markedly different from the $^{D}V/K$ values (cf. Tables 2 and 3). All effects are either equal to 1, within experimental error, or slightly inverse [^{D}V(C-2)]. These KIE measurements are consistent with the TS for V being associated with a different reaction step. Given that this step must come after those that limit V/K[23] and that the β_{lg} value on V is approximately zero, the first possible TS for V involves the hydration of the enzyme-bound glycal intermediate (k_9, Scheme 1). However, at present, given the lack of specific evidence, other subsequent steps in the mechanism, such as product release, might be kinetically significant for V.

CONCLUSIONS

The MelA α-galactosidase from *C. freundii* catalyzes hydrolysis of aryl substrates via a mechanism in which the first irreversible step (rate-limiting for V/K) involves oxidation of the C-3 hydroxyl group and proton abstraction at C-2, a process that starts before completion of the NAD^+-promoted hydride transfer. Subsequent elimination of the leaving group is kinetically silent, and this event is followed by hydration of the α,β-unsaturated enone intermediate. The catalytic cycle is completed by protonation at C-2 and reduction by the on-board NADH.

ASSOCIATED CONTENT

Supporting Information. Synthetic details for 1,2,3,4,6-penta-*O*-acetyl-D-[1-^{2}H]galactose, 4-nitrophenyl 6-phospho-α-D-galactoside (Schemes S1 and S2) and labeled galactal **7**, derivation of equations for the estimation of expected $^{D}V/K$(C-3,2-^{2}H) and $^{D}V/K$(C-2,3-^{2}H) values for a stepwise mechanism, Michaelis−Menten kinetic parameters for the MelA α-galactosidase-catalyzed hydrolysis of the seven aryl α-D-galactosides (Table S1), assay of reduced MelA (Figure S1), ligand binding curve for Mn^{2+} (Figure S2), pH dependence of k_{cat}/K_m for the MelA-catalyzed hydrolysis of 4NPαG (Figure S3), and ^{1}H and ^{13}C NMR spectra of labeled compounds **1b**−**e** and substrates **2b**−**f**. This material is available free of charge via the Internet at http://pubs.acs.org.

AUTHOR INFORMATION

Corresponding Author

*E-mail: bennet@sfu.ca. Telephone: (778) 782-8814. Fax: (778) 782-3765.

Funding Sources

This work was supported by the Natural Sciences and Engineering Research Council of Canada.

ABBREVIATIONS

[1-^{2}H]PαG, phenyl α-D-[1-^{2}H]galactoside; [2-^{2}H]PαG, phenyl α-D-[2-^{2}H]galactoside; [2,3-^{2}H$_2$]PαG, phenyl α-D-[2-^{2}H,-3-^{2}H]galactoside; [3-^{2}H]PαG, phenyl α-D-[3-^{2}H]galactoside; 4NPαG, 4-nitrophenyl α-D-galactoside; BSA, bovine serum albumin; DMAP, 4-(dimethylamino)pyridine; DTT, dithiothreitol; GH, glycosyl hydrolase; GH4, glycosyl hydrolase family 4; HEPES, 4-(2-hydroxyethyl)-1-piperazineethanesulfonic acid; IPTG, isopropyl 1-thio-β-D-galactopyranoside; KIE, kinetic isotope effect; NAD^+, β-nicotinamide adenine dinucleotide; NADH, reduced β-nicotinamide adenine dinucleotide; PαG, phenyl α-D-galactoside; PNP, *p*-nitrophenyl; TBDPS, *tert*-butyl diphenylsilyl; TCEP, tris(carboxyethyl)phosphine; THF, tetrahydrofuran; TLC, thin layer chromatography; Tris, tris(hydroxymethyl)aminomethane; TS, transition state; UV−vis, ultraviolet−visible.

REFERENCES

(1) Henrissat, B. (1991) A classification of glycosyl hydrolases based on amino acid sequence similarities. *Biochem. J. 280*, 309–316.

(2) Vocadlo, D. J., and Davies, G. J. (2008) Mechanistic insights into glycosidase chemistry. *Curr. Opin. Chem. Biol. 12*, 539–555.

(3) Rao, S. T., and Rossmann, M. G. (1973) Comparison of super-secondary structures in proteins. *J. Mol. Biol. 76*, 241–256.

(4) Lodge, J. A., Maier, T., Liebl, W., Hoffmann, V., and Strater, N. (2003) Crystal structure of *Thermotoga maritima* α-glucosidase AglA defines a new clan of NAD^+-dependent glycosidases. *J. Biol. Chem. 278*, 19151–19158.

(5) Liu, Q. Y. P. et al. (2007) Bacterial glycosidases for the production of universal red blood cells. *Nat. Biotechnol. 25*, 454–464.

(6) Yip, V. L. Y., and Withers, S. G. (2006) Mechanistic analysis of the unusual redox-elimination sequence employed by *Thermotoga maritima* BgIT: A 6-phospho-β-glucosidase from glycoside hydrolase family 4. *Biochemistry 45*, 571–580.

(7) Thompson, J., Pikis, A., Ruvinov, S. B., Henrissat, B., Yamamoto, H., and Sekiguchi, J. (1998) The gene *glvA* of *Bacillus subtilis* 168 encodes a metal-requiring, NAD(H)-dependent 6-phospho-α-glucosidase: Assignment to family 4 of the glycosylhydrolase superfamily. *J. Biol. Chem. 273*, 27347–27356.

(8) Coutinho, P. M., Deleury, E., Davies, G. J., and Henrissat, B. (2003) An evolving hierarchical family classification for glycosyltransferases. *J. Mol. Biol. 328*, 307–317.

(9) Yip, V. L. Y., Thompson, J., and Withers, S. G. (2007) Mechanism of GlvA from *Bacillus subtilis*: A detailed kinetic analysis of a 6-phospho-α-glucosidase from glycoside hydrolase family 4. *Biochemistry 46*, 9840–9852.

(10) Yip, V. L. Y. et al. (2004) An unusual mechanism of glycoside hydrolysis involving redox and elimination steps by a family 4 β-glycosidase from *Thermotoga maritima*. *J. Am. Chem. Soc. 126*, 8354–8355.

(11) Liljeström, P. L., and Liljeström, P. (1987) Nucleotide-sequence of the *MelA* gene, coding for α-galactosidase in *Escherichia coli* K-12. *Nucleic Acids Res. 15*, 2213–2220.

(12) Anggraeni, A. A., Sakka, M., Kimura, T., Ratanakhaokchai, K., Kitaoka, M., and Sakka, K. (2008) Characterization of *Bacillus halodurans* α-galactosidase Mel4A encoded by the *mel4A* gene (BH2228). *Biosci., Biotechnol., Biochem. 72*, 2459–2462.

(13) Sokolov, V. M., Zakharov, V. I., and Studentsov, E. P. (2002) Stereoselectivity of reactions at the glycoside center of carbohydrates: VII. Synthesis of aryl α- and β-D-glucopyranosides by Helferich, catalyzed by boron trifluoride etherate. *Russ. J. Gen. Chem. 72*, 806–811.

(14) Comfort, D. A. et al. (2007) Biochemical analysis of *Thermotoga maritima* GH36 α-galactosidase (*Tm*GalA) confirms the mechanistic commonality of Clan GH-D glycoside hydrolases. *Biochemistry 46*, 3319–3330.

(15) Lemieux, R. U., Nagabhushan, T. L., and O'Neill, I. K. (1964) A new approach to the synthesis of 2-amino-2-deoxyglycosides. *Tetrahedron Lett.*, 1909–1916.

(16) Taylor, J. R. (1982) *An introduction to error analysis: The study of uncertainties in physical measurements*, University Science Books, Mill Valley, CA.

(17) Lemieux, R. U., Nagabhushan, T. L., and Gunner, S. W. (1968) Synthesis of 3,4,6-tri-O-acetyl-2-oximino-α-D-hexopyranosides. *Can. J. Chem. 46*, 405–411.

(18) Czernecki, S., Vijayakumaran, K., and Ville, G. (1986) Convenient synthesis of hex-1-enopyran-3-uloses: Selective oxidation of allylic alcohols using pyridinium dichromate. *J. Org. Chem. 51*, 5472–5475.

(19) Fujiwara, T., and Hayashi, M. (2008) Efficient synthesis of rare sugar D-allal via reversal of diastereoselection in the reduction of protected 1,5-anhydrohex-1-en-3-uloses: Protecting group dependence of the stereoselection. *J. Org. Chem. 73*, 9161–9163.

(20) Hermes, J. D., Roeske, C. A., O'Leary, M. H., and Cleland, W. W. (1982) Use of multiple isotope effects to determine enzyme mechanisms and intrinsic isotope effects. Malic enzyme and glucose-6-phosphate dehydrogenase. *Biochemistry 21*, 5106–5114.

(21) Cook, P. F., and Cleland, W. W. (2007) *Enzyme kinetics and mechanism*, Garland Science, London.

(22) Cook, P. F., Blanchard, J. S., and Cleland, W. W. (1980) Primary and secondary deuterium isotope effects on equilibrium constants for enzyme-catalyzed reactions. *Biochemistry 19*, 4853–4858.

(23) Fersht, A. (1985) *Enzyme structure and mechanism*, 2nd ed., W. H. Freeman, New York.